

Synthesis of Mn₃O₄ Microflowers Anode Material for Lithium-ion Batteries with Enhanced Performance

Hai L. Fei^{1,2*} and Cao Yang¹

¹State Key Laboratory of Photocatalysis on Energy and Environment, College of Chemistry, Fuzhou University, Fuzhou, Fujian 350002, China.

²Key Laboratory of Advanced Energy Materials Chemistry (Ministry of Education), Nankai University, Tianjin 300071, China.

Short Research Article

ABSTRACT

It is important to prepare novel micro-nanostructures of Mn-based oxides for energy storage. In this study, a simple and versatile method for preparation of Mn₃O₄ microflowers associated with super-thin nanosheets has been developed via a solvo-thermal approach in the presence of a surfactant hexadecyl trimethyl ammonium bromide (CTABr). Mn₃O₄ nanoparticles can be selectively prepared without organic solvents and surfactants. When tested as a new high-capacity anode material for lithium-ion batteries, Mn₃O₄ microflowers showed better cycling performance than Mn₃O₄ nanoparticles. The Mn₃O₄ microflowers-based composite electrode delivered a second discharge capacity of 870.2 mA h g⁻¹ at a current density of 240 mA g⁻¹. While the Mn₃O₄ nanoparticle-based composite electrode delivered a second discharge capacity of 332.8 mA h g⁻¹. The improved discharge capacity and cycling performance occurred as the Mn₃O₄ microflower did not undergo reduction from Mn(III) to Mn(II) in the discharge process and it also reduced polarisation. Research on this topic mainly shed some light on the preparation of three-dimensional flower-like oxide hierarchical architectures with an improved electrochemical performance for energy storage.

Keywords: Manganese oxide; Hierarchical architectures; Anode; Lithium-ion battery; Surfactant; Nanosheet.

1. INTRODUCTION

Rechargeable batteries with reversible and efficient electrochemical energy storage and conversion are urgent in various applications, such as portable electronic consumer devices, electric vehicles, and large-scale electricity storage in smart and intelligent grids as renewable and clean energy [1, 2]. Lithium-ion battery is one of the fascinating rechargeable batteries for high energy density, coupled with a long life cycle and charge-discharge rate capability [3]. Studies have been conducted to develop low-cost, sustainable, renewable, safe, and high-energy density electrode materials for lithium-ion batteries. Considering environmental safety, researchers should prepare potential

electrode materials for lithium-ion batteries through green chemistry based on inexpensive and straightforward procedures.

Manganese-based anode materials are less toxic, abundant in natural resources [4]. Though Mn₃O₄ is isostructural with Co₃O₄, it has poor lithiation activity and electrically insulating, resulting in fast capacity decay as anode materials for lithium-ion batteries. Recently significant progress has been achieved for Mn₃O₄ anode materials. The improved electrochemical properties turned true via the following methods. Mesoporous carbon, graphene, carbon nanotube and various carbon nanostructures were introduced to prepare carbon based Mn₃O₄ nano-composites. These composites showed better

*Corresponding author: Email: hailongfei@fzu.edu.cn;

cycling stability and higher discharge capacity than bulk Mn_3O_4 for fast ion diffusion, good electronic conductivity, and skeleton supporting function [5-35]. People also designed various Mn_3O_4 nanostructures to improve the cycling performance of Mn_3O_4 . In these Mn_3O_4 nanostructures, well-shaped nanostructure, pore, hollow structure and 3D array played an important role in the long cycling performance. Novel spongelike nanosized Mn_3O_4 exhibits a high initial reversible capacity of 869 mA h g^{-1} and significantly enhanced first coulomb efficiency with a stabilised reversible capacity of around 800 mA h g^{-1} after more than 40 charge/discharge cycles [4]. Mn_3O_4 hollow microspheres demonstrate a good electrochemical performance, with a high reversible capacity of $646.9 \text{ mA h g}^{-1}$ after 240 cycles at a current density of 200 mA h g^{-1} [36], while fluorinated Mn_3O_4 nanospheres for lithium-ion batteries show poor cycling performances [37]. 3D porous Mn_3O_4 nanosheet arrays could be directly used as a binder-free and conductive-agent-free electrode to deliver ultrahigh electrochemical performance [38]. It has been reported that the 3D pores and voids between the nanosheet arrays could provide rapid ion transfer channels, as well as accommodating the volumetric changes of Mn_3O_4 during the electrochemical cycling [38]. The ultrathin Mn_3O_4 nanosheets exhibit a high reversible capacity and stronger cycling stability for the high surface area [39]. The well-shaped Mn_3O_4 tetragonal bipyramids with high-energy facets show a high initial discharge capacity. Besides, the anode displays a fast performance and delivers a reversible capacity of $822.3 \text{ mA h g}^{-1}$ (the theoretical capacity: 937 mA h g^{-1} at a current density of 0.2 C after 50 cycles [40]. The porous Mn_3O_4 nano rods can improve electrochemical reaction kinetics and favour the formation of Mn_3O_4 [41]. Mn_3O_4 nano-octahedra has a discharge capacity of $667.9 \text{ mA h g}^{-1}$ after 1000 cycles at 1.0 A g^{-1} ascribed to the lower charge transfer resistance due to the exposed highly active {011} facets. This can facilitate the conversion reaction of Mn_3O_4 and Li owing to the alternating Mn and O atom layers, resulting in easy formation and decomposition of the amorphous Li_2O and the multi-electron reaction [42]. The hollow Mn_3O_4 spheres deliver a highly stable cycle performance with capacity retention of similar to 980 mA h g^{-1} for over 140 cycles at 200 mA g^{-1} and an excellent rate capability [43]. It can be seen that Mn_3O_4 with nanosheets, pore, high surface area and interconnected voids are suitable to show high discharge capacity and long cycling stability. The 3D Mn_3O_4 microflowers

assembling with nanosheets are expected to show favourable electrochemical performances for the presence of voids among the nanosheet arrays. There are few reports on the research of Mn_3O_4 microflowers except $\text{Mn}_3\text{O}_4\text{-Fe}_3\text{O}_4$ and $\text{MnO-Mn}_3\text{O}_4$ nanoflowers. $\text{Mn}_3\text{O}_4\text{-Fe}_3\text{O}_4$ nanoflowers are simply fabricated through one step etching $\text{Mn}_5\text{Fe}_5\text{Al}_{90}$ ternary alloy, which exhibits higher performance as anode material for lithium-ion batteries than that of pure Mn_3O_4 and Mn_3O_4 anodes for unique hierarchical flower-like structure and the synergistic effects between Mn_3O_4 and Mn_3O_4 [44]. A hierarchically porous $\text{MnO-Mn}_3\text{O}_4$ nano-flowers can be fabricated by dealloying Mn/Al alloys in aqueous NaOH solution in the presence of H_2O_2 , and upon annealing, which has a capacity of 1018, 901 and 757 mA h g^{-1} with nearly 100% retention capacity after 100 cycles at 100, 200 and 500 mA g^{-1} [45]. Mn_3O_4 nanosheets associated with nanorods can be assembled to 3D flower-like Mn_3O_4 with hexadecyl trimethyl ammonium bromide (CTABr), urea and MnSO_4 as reagents, while they did not test any properties, e.g. batteries [46].

In this study, a simple method was developed to prepare Mn_3O_4 microflowers associated with nanosheets. These microflowers were synthesised in a N,N-dimethylformamide (DMF)-water solution with the aid of CTABr. When tested as an anode material for lithium-ion batteries, the Mn_3O_4 microflowers exhibited enhanced cycling stability than Mn_3O_4 nanoparticles.

2. MATERIALS AND METHODS

All commercially available chemicals were used for the study. The preparation was performed via a solvothermal method in a DMF-water mixed solvent. In a typical procedure, 1 mmol manganese acetate tetrahydrate and 0.5 g hexadecyl trimethyl ammonium bromide (CTABr) were added to a 5 ml DMF- 25 ml water solution and stirred at room temperature for 2 hours. After that, the mixture was transferred to a 50-ml Teflon-lined stainless autoclave, sealed, kept at 200° C for 24 hours and then cooled to room temperature. It was then washed with absolute alcohol and dried at 70° C for 12 hours (marked with DT-1). Sample DT-2 was prepared without CTABr under the identical condition, while sample DT-3 was prepared with 30 ml water in the absence of CTABr.

The morphological characteristics of the as-synthesised materials were observed with a

Comment [Ed2]: Incorrect use of verb

Comment [Ed1]: Avoid making very long sentence in scientific writing.

Hitachi S-4800 field emission scanning electron microscope (SEM). X-ray diffraction (XRD) patterns were recorded on a diffract meter (Co K α , Analytical, and Pert). Cyclic voltammetry (CV) experiments were performed with a Chi660c electrochemical work station at a scan rate of 1 mV S⁻¹. A Land CT2001A battery tester was used to measure the electrode activities at room temperature.

The as-synthesised samples were tested as anode materials for lithium-ion batteries. The composite of the negative electrode material was consisted of the active material, a conductive material (super-pure carbon) and binder polyvinylidene difluoride (PVDF) in a weight ratio of 7/2/1. The Li metal was used as the counter electrode. The cells were charged and discharged between a 0.05 - 3.0 V voltage limit.

3. RESULTS AND DISCUSSION

Three samples were obtained by adjusting synthesis parameters. Both DMF and CTABr play an important role in the formation of different morphologies. When water was used as the solvent in the absence of CTABr, the sample appeared as monodispersed nanoparticles between 30 and 150 nm in Fig. 1a, b. As shown in Fig. 1c, d, when DMF was added, thin microplatelets were obtained. The length and width of microplatelets can be up to several μm . There are also some thin nanobelts. Some microflowers composed of superimposed thin and wide nanosheets were prepared with CTABr in the DMF-H₂O mixed solvent in Fig. 1e, f. Certain microflower is several μm in size.

XRD was performed to identify the structure of the three samples. It can be seen that CTABr played an important role in the crystallisation of products. The diffraction peaks of the sample prepared with DMF, water and CTABr had the highest intensity than samples prepared with water, CTABr and DMF (Fig. 2). The diffraction peaks can be ascribed to Mn₃O₄ in Fig. 2a (JCPDS 89-4837). The other samples can also be ascribed to Mn₃O₄ as can be seen in Fig. 2b, c,. All the Mn₃O₄ showed lack of the peak of (101), which means that it was not the high-energy {101} plane.

The electrochemical performance of Mn₃O₄ nanoparticles and microflowers was evaluated as anode materials for lithium-ion batteries (Fig. 3). Fig. 3a shows the 1st and 2nd charge-discharge profiles of Mn₃O₄ microflowers at a current density of 240 mA g⁻¹ (Sample T-72). A long

discharge platform is observed at 0.5 V in the first discharge curve, but this platform disappears in the succeeding discharge curves. The Mn₃O₄ microflowers-based composite electrode delivers an initial discharge capacity of 1496 mA h g⁻¹. However, the 1st discharge profiles of Mn₃O₄ nanoparticles showed four discharge platforms at 0.33, 0.44, 0.92 and 1.3 V, implying the occurrence of a multi-step conversion reaction. A new platform at 0.7 V appeared in the succeeding discharge curves. The Mn₃O₄ nanoparticles-based composite electrode delivered an initial discharge capacity of 1280 mA h g⁻¹. It can be seen that Mn₃O₄ without high-energy {101} plane can also have a very high initial discharge capacity. It can also be found that Mn₃O₄ nanoparticles have a steeper charge curve than Mn₃O₄ microflowers between 1.4 and 3.0 V implying that a severe polarisation takes place in the Mn₃O₄ nanoparticles-based composite electrode.

Figs. 4 and 5 display the dQ/dV-V curves obtained from the 1st and 2nd charge-discharge curves of Mn₃O₄ nanoparticles and microflowers. In the first charge-discharge cycle of Mn₃O₄ nanoparticles, four reduction peaks are centered at 0.33, 0.45, 0.90 and 1.3 V, and the oxidation peak is at 1.24 V as shown in Fig. 4a. In the first charge-discharge cycle of Mn₃O₄ microflowers, the reduction and oxidation peaks were centered at 0.33 and 1.28 V (Fig. 4b), respectively. In the second charge-discharge cycle of Mn₃O₄ nanoparticles, two reduction peaks were centered at 0.45 and 0.52 V, and the oxidation peak was at 1.24 V (Fig. 5b). In the second charge-discharge cycle of Mn₃O₄ microflowers, the reduction and oxidation peaks were centered at 0.54 and 1.25 V (Fig. 5a), respectively. The reduction peaks in the range of 1.3-0.4 V was ascribed to reduction from Mn(III) to Mn(II), and the 0.4-0.1 V range reflected the reduction from Mn(II) to Mn(0) [47,48]. The difference of first discharge curve between Mn₃O₄ microflowers and nanoparticles is because Mn₃O₄ microflowers only undergoes the reduction from Mn(II) to Mn(0). While Mn₃O₄ nanoparticles undergo reductions from Mn(III) to Mn(II) to Mn(0). In the second discharge, the contribution to discharge capacity is mainly ascribed to the reduction around 0.5 V. The Li⁺ charge reaction: is Mn₃O₄ + 8Li⁺ + 8e⁻ to 3Mn(0) + 8Li₂O [49]. Compared to Mn₃O₄ nanoparticles, Mn₃O₄ microflowers does not undergo reduction from Mn(III) to Mn(II) and reduce polarisation.

Fig. 6 shows the cycling performance tested at current densities of 240 and 480 mA g⁻¹. The

Comment [Ed3]: This term has already been associated with its acronym, so just use the acronym.

Comment [Ed4]: When this term Fig. is used at the beginning of a sentence, it is spelled out.

Mn₃O₄ microflowers-based composite electrode delivered a second discharge capacity of 870.2 and 714.8 mA h g⁻¹ as shown in Fig. 6a,b, respectively. A reversible capacity of 392.8 and

358.5 mA h g⁻¹ was retained after 20 cycles. The Mn₃O₄ nanoparticles-based composite electrode showed lower discharge capacity and worse cycling stability at current densities of 240 and

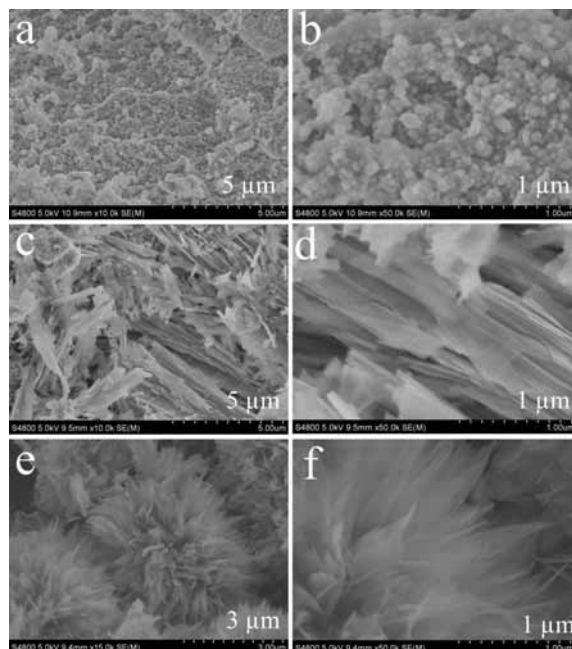


Fig. 1. SEM images of samples with (a, b) water, (c, d) water and DMF, and (e, f) water, DMF and CTABr

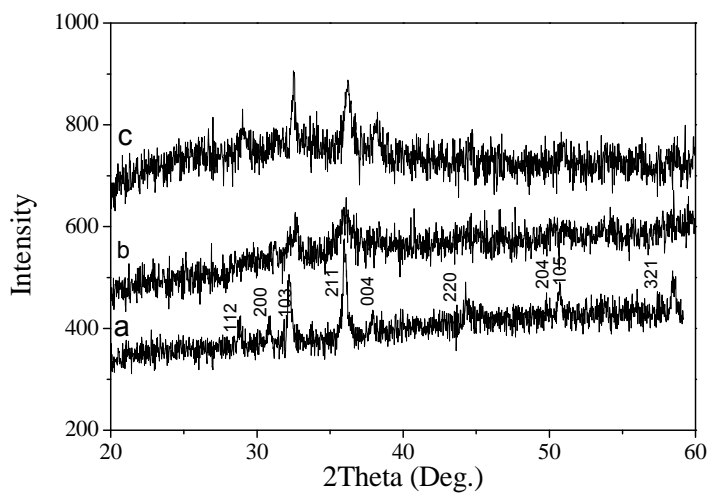


Fig. 2. Wide angle XRD patterns of samples with (a) water, DMF and CTABr, (b) water and DMF, and (c) water

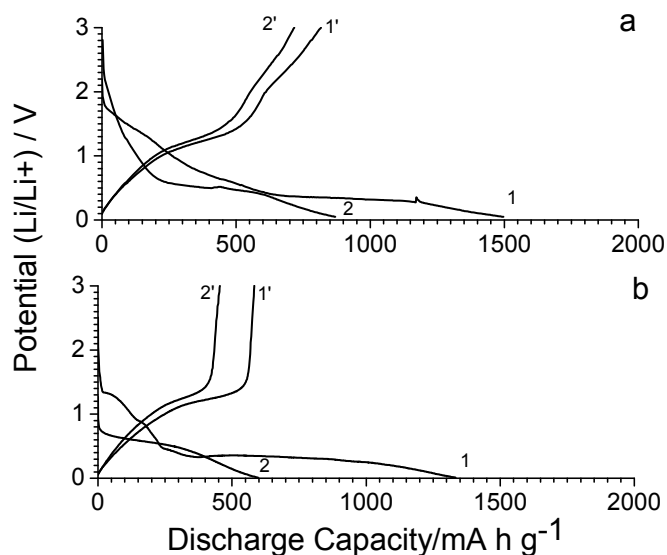


Fig. 3. The first and second charge-discharge profiles at a current density of 240 mA g⁻¹ of (a) Mn₃O₄ microflowers and (b) Mn₃O₄ nanoparticles

480 mA g⁻¹ as can be seen from Fig. 6c,d. It delivered a second discharge capacity of 332.8 and 156.5 mA h g⁻¹, respectively. The final discharge capacity was even low to 131.3 and 53.8 mA h g⁻¹. The fast capacity decay of Mn₃O₄ nanoparticles is due to the reduction from Mn(III) to Mn(II). The improved electrochemical performance of Mn₃O₄ microflowers is due to the reduced activity of Mn₃O₄, avoiding the complicated reduction from Mn(III) to Mn(II) and

reduced polarisation. The present study focused on the research of flower-like rutile TiO₂ and ammonium vanadium bronze. It was found that the effect of flower-like nanostructures on the reaction kinetics of the electrode are ascribed to the changes the total impedance and electron transfer resistance [50, 51]. The improved performance of Mn₃O₄ micro-flowers is also ascribed to improve the transferring of electron.

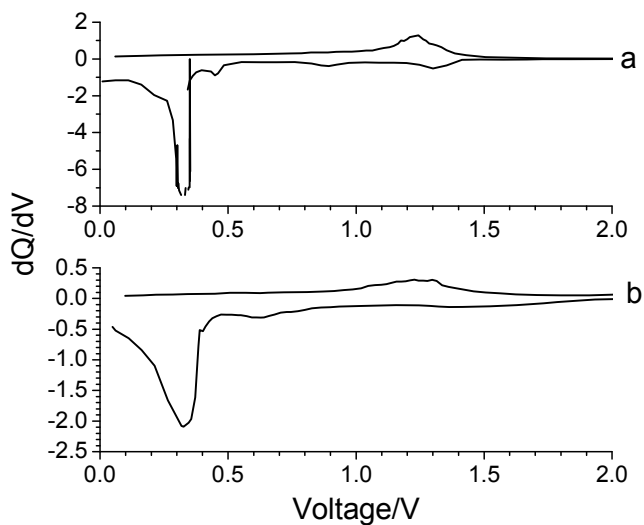


Fig. 4. The dQ/dV-curve derived the first charge-discharge profiles of (a) Mn₃O₄ nanoparticles (b) Mn₃O₄microflowers

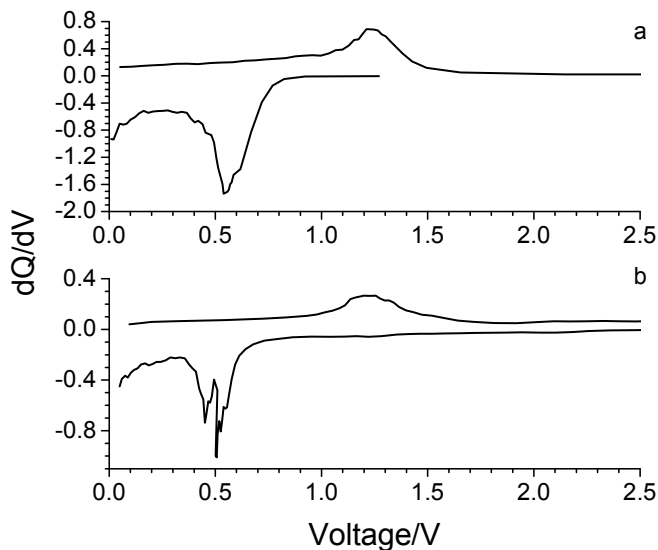


Fig. 5. The dQ/dV-curve derived the second charge-discharge profiles of (a) Mn₃O₄ microflowers (b) Mn₃O₄ nanoparticles

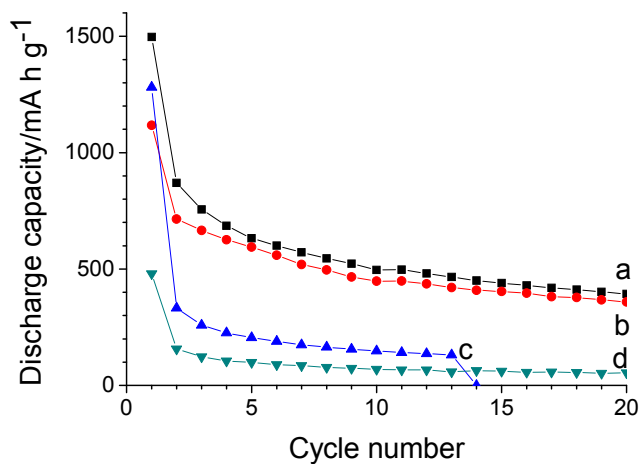


Fig. 6. The cyclic performance tested at current densities of 240 and 480 mA g⁻¹ of (a, b) Mn₃O₄ microflowers, and (c, d) Mn₃O₄ nanoparticles

4. CONCLUSION

In summary, the controlled synthesis of Mn₃O₄ microflowers associated with super-thin

nanosheets was achieved via using a solvothermal method with the aid of surfactant CTABr. The solvent plays an important role in the morphology of Mn₃O₄. Mn₃O₄ nanoparticles were

prepared with water as a solvent, while Mn₃O₄ microplatelets were obtained with DMF via affecting nucleation. The surfactant CTABr directed the formation of Mn₃O₄ microflowers from platelet-like precursors. The Mn₃O₄ microflowers exhibited better cycling stability and higher discharge capacity than Mn₃O₄ nanoparticles as anode materials for lithium-ion batteries. It is due to the reduced activity of Mn₃O₄, avoiding the complicated reduction from Mn(III) to Mn(II) and reduced polarisation. It can be said that this simple method may also be used to fabricate other anode materials for lithium-ion batteries with improved electrochemical performance.

COMPETING INTERESTS

Authors have declared that no competing interests exist.

REFERENCES

- Cheng FY, Liang J, Tao ZL, Chen J. Functional materials for rechargeable batteries. *Adv Mater.* 2012;23:1695-1715.
- Fei HL, Liu X, Li ZW. Hollow cobalt coordination polymer microspheres: a promising anode material for lithium-ion batteries with high performance. *Chem Eng J.* 2015;281:453-458.
- Tarascon JM. Key challenges in future Li-battery research. *Phil. Trans. R. Soc. A.* 2010;368:3227-3241.
- Gao J, Lowe MA, Abruña HD, Spongelike nanosized Mn₃O₄ as a high-capacity anode material for rechargeable lithium batteries. *Chem Mater.* 2011;23:3223-3227.
- Zhang LP, Li GS, Fan JM, Li BY. In situ synthesis of Mn₃O₄ nanoparticles on hollow carbon nanofiber as high-performance lithium ion battery anode. *Chem.* 2018;DOI:10.1002/chem.201801196.
- Guo LG, Ding Y, Qin CQ et al, Anchoring Mn₃O₄ nanoparticles onto nitrogen-doped porous carbon spheres derived from carboxymethyl chitosan as superior anodes for lithium-ion batteries. *J Alloy Compd.* 2018;735:209-217.
- Song NJ, Ma CL. A green synthesis of Mn₃O₄/graphene nanocomposite as anode material for lithium-ion batteries. *Int J Electrochem Sci.* 2018;13:452-460.
- Wu LL, Zhao DL, Cheng XW, Ding ZW, Hu T, Meng S. Nanorod Mn₃O₄ anchored on graphene nanosheet as anode of lithium ion batteries with enhanced reversible capacity and cyclic performance. *J Alloy Compd.* 2018;728:383-390.
- Li Z, Tang B, Mn₃O₄/nitrogen-doped porous carbon fiber hybrids involving multiple covalent interactions and open voids as flexible anodes for lithium-ion batteries. *Green Chem.* 2017;19:5862-5873.
- Liu BB, Qi L, Ye JJ, Wang JQ, Xu CX. Facile fabrication of graphene-encapsulated Mn₃O₄ octahedra cross-linked with a silver network as a high-capacity anode material for lithium ion batteries. *New J Chem.* 2017;41:13454-13461.
- Peng HJ, Hao GX, Chu ZH, Lin J, Lin XM, Cai YP. Mesoporous Mn₃O₄/C microspheres fabricated from MOF template as advanced lithium-ion battery anode. *Crys Growth & Des.* 2017;11:5881-5886.
- Lv KK, Zhang YH, Zhang DY, Ren WW, Sun L. Mn₃O₄ nanoparticles embedded in 3D reduced graphene oxide network as anode for high-performance lithium ion batteries. *J Mater Sci-Mater. El.,* 2017;28:14919-14927.
- Pramanik A, Maiti S, Sreemany M, Mahanty S. Rock-salt-templated Mn₃O₄ nanoparticles encapsulated in a mesoporous 2D carbon matrix: a high rate 2 V anode for lithium-ion batteries with extraordinary cycling stability. *Chemistryselect,* 2017;2:854-7864.
- Zhang R, Wang D, Qin LC, MnCO₃/Mn₃O₄/reduced graphene oxide ternary anode materials for lithium-ion batteries: facile green synthesis and enhanced electrochemical performance. *J Mater Chem A,* 2017;5:17001-17011.
- Zhuang YC, Ma Z, Deng YM, Song XN, Zuo XX, Xiao X, Nan JM. Sandwich-like Mn₃O₄/carbon nanofragment composites with a higher capacity than commercial graphite and hierarchical voltage plateaus for lithium ion batteries. *Electrochim Acta.* 2017;440-447.
- Yang ZL, Lu DL, Zhao RR, Gao AM, Chen HY. Synthesis of a novel structured Mn₃O₄@C composite and its performance as anode for lithium ion battery. *Mater Lett.* 2017;198:97-100.
- Cui X, Wang YQ, Xu QY, Sun P, Wang XZ, Wei T, Sun YM. Carbon nanotube entangled Mn₃O₄ octahedron as anode

- materials for lithium-ion batteries. *Nanotech.* 2017;28:255402.
18. Chen JY, Wu XF, Gong Y, Wang PF, Li WH, Tan QQ, Chen YF. Synthesis of Mn_3O_4 /N-doped graphene hybrid and its improved electrochemical performance for lithium-ion batteries. *Ceram Int.* 2017;43:4655-4662.
 19. Gangaraju D, Sridhar V, Lee I, Park H. Graphene - carbon nanotube - Mn_3O_4 mesoporous nano-alloys as high capacity anodes for lithium-ion batteries. *J Alloy Compd.* 2017;699:106-111.
 20. Seong CY, Park SK, Bae Y, Yoo S, Piao Y. An acid-treated reduced graphene oxide/ Mn_3O_4 nanorod nanocomposite as an enhanced anode material for lithium ion batteries. *Rsc Adv.* 2017;7:37502-37507.
 21. Park I, Kim T, Park H, Mun M, Shim SE, Baek SH. Preparation and electrochemical properties of Pt-Ru/ Mn_3O_4 /C bifunctional catalysts for lithium-air secondary battery. *J Nanosci. Nanotechnol.* 2016;16:10453-10458.
 22. Zhang Y, Yue KQ, Zhao HS, Wu Y, Duan LF, Wang KL. Bovine serum albumin assisted synthesis of Fe_3O_4 @C@ Mn_3O_4 multilayer core-shell porous spheres as anodes for lithium ion battery. *Chem Eng J.* 2016;291:238-243.
 23. Park SK, Seong CY, Yoo S, Piao Y. Porous Mn_3O_4 nanorod/reduced graphene oxide hybrid paper as a flexible and binder-free anode material for lithium ion battery. *Energy.* 2016;99:266-273.
 24. Alfuruqi MH, Gim J, Kim S, Song J, Duong PT, Jo J, Baboo JP, Xiu Z, Mathew V, Kim J. One-step pyro-synthesis of a nanostructured Mn_3O_4 /C electrode with long cycle stability for rechargeable lithium-ion batteries. *Chem-A Eur J.* 2016;22:2039-2045.
 25. Bhimanapati G, Yang RG, Robinson JA, Wang Q. Effect of Mn_3O_4 nanoparticle composition and distribution on graphene as a potential hybrid anode material for lithium-ion batteries. *Rsc Adv.* 2016;6:33022-33030.
 26. Jing MJ, Wang JF, Hou HS, Yang YC, Zhang Y, Pan CC, Chen J, Zhu YR, Ji XB. Carbon quantum dot coated Mn_3O_4 with enhanced performances for lithium-ion batteries. *J Mater Chem A.* 2015;3:16824-16830.
 27. Ren YR, Wang JW, Huang XB, Yang B, Ding JN. One step hydrothermal synthesis of Mn_3O_4 /graphene composites with great electrochemical properties for lithium-ion batteries. *Rsc Adv.* 2015;5:59208-59217.
 28. Yue HW, Li F, Yang ZB, Li XW, Lin SM, He DY. Facile preparation of Mn_3O_4 -coated carbon nanofibers on copper foam as a high-capacity and long-life anode for lithium-ion batteries. *J Mater Chem A.* 2014;2:17352-17358.
 29. Luo S, Wu HC, Wu Y, Jiang KL, Wang JP, Fan SS. Mn_3O_4 nanoparticles anchored on continuous carbon nanotube network as superior anodes for lithium ion batteries. *J Power Sources.* 2014;249:463-469.
 30. Park SK, Jin A, Yu SH, Ha J, Jang B, Bong S, Woo S, Sung YE, Piao Y. In situ hydrothermal synthesis of Mn_3O_4 nanoparticles on nitrogen-doped graphene as high-performance anode materials for lithium ion batteries. *Electrochim Acta.* 2014;120:452-459.
 31. Luo YQ, Fan SS, Hao NY, Zhong SL, Liu WC. An ultrasound-assisted approach to synthesize Mn_3O_4 /RGO hybrids with high capability for lithium ion batteries. *Dalton T.* 2014;43:15317-15320.
 32. Lavoie N, Malenfant PRL, Courtel FM, Abu-Lebdeh Y, Davidson IJ. High gravimetric capacity and long cycle life in Mn_3O_4 /graphene platelet/LiCMC composite lithium-ion battery anodes. *J Power Sources.* 2012;213:249-254.
 33. Wang ZH, Yuan LX, Shao QG, Huang F, Huang YH. Mn_3O_4 nanocrystals anchored on multi-walled carbon nanotubes as high-performance anode materials for lithium-ion batteries. *Mater Lett.* 2012;80:110-113.
 34. Wang CB, Yin LW, Xiang D, Qi YX. Uniform carbon layer coated Mn_3O_4 nanorod anodes with improved reversible capacity and cyclic stability for lithium ion batteries. *ACS Appl Mater Inter.* 2012;4:1636-1642.
 35. Li ZQ, Liu NN, Wang XK, Wang CB, Qi YX, Yin LW. Three-dimensional nanohybrids of Mn_3O_4 /ordered mesoporous carbons for high performance anode materials for lithium-ion batteries. *J Mater Chem.* 2012;22:16640-16648.
 36. Palaniyandy N, Nkosi FP, Raju K, Ozoemena KI. Fluorinated Mn_3O_4 nanospheres for lithium-ion batteries: Low-cost synthesis with enhanced capacity, cyclability and charge-transport. *Mater Chem Phys.* 2018;209:65-75.
 37. Jiang Z, Huang KH, Yang D, Wang S, Zhong H, Jiang CW. Facile preparation of Mn_3O_4 hollow microspheres via reduction of pentachloropyridine and their

- performance in lithium-ion batteries. *RSC Adv.* 2017;3:8264-8271.
38. Fan XY, Cui Y, Liu P, Gou L, Xu L, Li DL. Electrochemical construction of three-dimensional porous Mn_3O_4 nanosheet arrays as an anode for the lithium ion battery. *Phys Chem Chem Phys.* 2016;18:22224-22234.
 39. Zhen MM, Zhang Z, Ren QT, Liu L. Room-temperature synthesis of ultrathin Mn_3O_4 nanosheets as anode materials for lithium-ion batteries. *Mater Lett.* 2016;177:21-24.
 40. Li TT, Guo CL, Sun B, Li T, Li YG, Hou LF, Wei YH. Well-shaped Mn_3O_4 tetragonal bipyramids with good performance for lithium ion batteries. *J Mater Chem A.* 2015;3:7248-7254.
 41. Bai ZC, Zhang XY, Zhang YW, Guo CL, Tang B. Facile synthesis of mesoporous Mn_3O_4 nanorods as a promising anode material for high performance Lithium-ion batteries. *J Mater Chem A.* 2014;2:16755-16760.
 42. Huang SZ, Jin J, Cai Y, Li Y, Tan HY, Wang HE, Tendeloo GV, Su BL. Engineering single crystalline Mn_3O_4 nanooctahedra with exposed highly active {011} facets for high performance lithium ion batteries. *Nanoscale.* 2014;6 : 6819-6827.
 43. Jian GQ, Xu YH, Lai LC, Wang CS, Zachariah MR. Mn_3O_4 hollow spheres for lithium-ion batteries with high rate and capacity. *J Mater Chem A.* 2014;2:4627-4632.
 44. Zhao DY, Hao Q, Xu CX, Facile fabrication of composited Mn_3O_4/Fe_3O_4 nanoflowers with high electrochemical performance as anode material for lithium ion batteries. *Electrochim Acta.* 2015;180:493-500.
 45. Wang JZ, Du N, Wu H, Zhang H, Yu JX, Yang DR, Order-aligned Mn_3O_4 nanostructures as super high-rate electrodes for rechargeable lithium-ion batteries. *J. Power Sources.* 2013;222:32-37.
 46. Wang M, Cheng LM, Li QB, Chen ZW, Wang SL. Two-dimensional nanosheets associated with one-dimensional single-crystalline nanorods self-assembled into three-dimensional flower-like Mn_3O_4 hierarchical architectures. *Phys Chem Chem Phys.* 2014;39:21742-21746.
 47. Pasero D, Reeves N, West AR, Co-doped Mn_3O_4 : a possible anode material for lithium batteries. *J Power Sources.* 2005;141:156-158.
 48. Wang HL, Cui LF, Yang Y, Casalongue HS, Robinson JT, Liang YY, Cui Y, Dai HJ. Mn_3O_4 -graphene hybrid as a high-capacity anode material for lithium ion batteries. *J Am Chem Soc.* 2010;132:13978-13980.
 49. Wu Z, Ren W, Wen L, Gao L, Zhao J, Chen Z, Zhou G, Li F, Cheng H. Graphene anchored with Co_3O_4 nanoparticles as anode of lithium ion batteries with enhanced reversible capacity and cyclic performance. *ACS Nano.* 2010;4:3187-3194.
 50. Fei HL, Wei MD. Facile synthesis of hierarchical nanostructured rutile titania for lithium-ion battery. *Electrochim Acta.* 2011;56: 6997-7004.
 51. Fei HL, Li H, Li ZW, Feng WJ, Liu X, Wei MD. Facile synthesis of graphite nitrate-like ammonium vanadium bronzes and their graphene composites for sodium-ion battery cathodes. *Dalton Trans.* 2014; 43: 16522-16527.